Progress in Organic Coatings 78 (2015) 21–27

Contents lists available at ScienceDirect

Progress in Organic Coatings

journal homepage: www.elsevier.com/locate/porgcoat

Electrodeposition of bilayered polypyrrole on 316 L stainless steel for corrosion prevention

M.B. González, S.B. Saidman*

Instituto de Ingeniería Electroquímica y Corrosión (INIEC), Departamento de Ingeniería Química, Universidad Nacional del Sur, Av. Alem 1253, B8000CPB Bahía Blanca, Argentina

ARTICLE INFO

Article history:
Received 8 July 2014
Received in revised form 16 October 2014
Accepted 23 October 2014

Keywords:
Polymers
Coatings
Electrochemical techniques
Corrosion

ABSTRACT

The electropolymerization of pyrrole in aqueous solutions of salicylate leads to the formation of hollow rectangular-sectioned microtubes. With the aim to develop a coating with this morphology but with better anticorrosive properties we synthesized a bilayer system by depositing a polypyrrole underlayer electropolymerized in the presence of molybdate and nitrate and a polypyrrole film formed by the microtubes as a top layer. The corrosion performance of the coatings was monitored by following the open circuit potentials, polarization curves and electrochemical impedance spectroscopy in acid and neutral chloride solutions. The bilayers have the capacity to protect the steel against uniform as well as against pitting corrosion during long exposure times. The system with the inner layer formed in alkaline solution was the most protective coating in this study. The results are discussed in terms of the galvanic interaction between the polymer and the substrate and the role played by the dopant anions.

1. Introduction

There has been a great interest in the synthesis of micro- and nanostructures of polypyrrole (PPy) due to their applications in many fields such as sensors [1], supercapacitors [2], biomedicine [3], and smart coatings [4]. In particular, the chemical synthesis of hollow microtubes with a rectangular cross-section has been reported [5]. This interesting morphology presents unique properties principally associated with its high exposed surface area. As was shown in our earlier works, the electrosynthesis of hollow rectangular microtubes of PPy can be performed in neutral or alkaline solutions of salicylate (Sa) [6]. It was postulated that as a result of the local pH decrease during electropolymerization, salicylic acid (HSa) crystallizes on the electrode surface and then the polymer is deposited on the external surface of these crystals [6,7]. The rectangular structures are constituted by both HSa and oxidized PPy doped with Sa anions. As an application, the PPy coating constituted by rectangular microtubes can be used for drug storage. Active agents can be entrapped during the electropolymerization into the conducting polymer matrix or can be immobilized in a later step [8–10]. In our previous work, Ag species were successfully immobilized in the PPy coating electrosynthesized in Sa solution and the modified electrode presented a very good performance toward inhibition of bacteria activity [11].

On the other hand, conducting polymers are intensively investigated for their use in corrosion protection applications [12–14]. A previous study proved that a PPy film formed in alkaline or neutral media containing MoO_4^{2-} and NO_3^- exhibits very good corrosion protection properties [15]. Both anions, which are efficient corrosion inhibitors for iron-based materials, are incorporated in the PPy matrix as dopants. The best performance corresponds to the film synthesized at pH 12.

Films should be uniform and pore-free. In spite of the passivation ability of conducting polymers, the presence of defects and pores may allow the electrolyte to reach the metallic substrate, triggering the corrosion process [16,17]. The corrosion resistance of the film constituted by hollow rectangular microtubes coating is not very high enough due to the opened structure [18]. This fact is a limiting factor for the applications of this coating. An attractive alternative to improve the corrosion protection of the substrate is the synthesis of PPy in the presence of MoO_4^{2-} and NO_3^- followed by the electropolymerization of PPy in Sa solutions. Results of this electropolymerization process and the evaluation of the steel protection against corrosion using the electrodeposited coatings are presented in this work.

* Corresponding author. Tel.: +54 291 4595182; fax: +54 291 4595182.
E-mail address: ssaidman@criba.edu.ar (S.B. Saidman).

http://dx.doi.org/10.1016/j.porgcoat.2014.10.012
0300-9440/

2. Experimental

The working electrode was a disk of stainless steel 316 L (316 L SS) mounted in a Teflon holder with an exposed area of 0.070 cm^2. Its chemical composition (wt.%) is: 17.47 Cr, 10.32 Ni, 1.88 Mn, 1.90 Mo, 0.39 Si, 0.025 C and Fe balance. The 316 L SS electrodes were polished with 1200 using SiC, then degreased with acetone and washed with triply distilled water. Immediately after, the electrode was transferred to the electrochemical cell.

A conventional three electrode system was used for the electrochemical experiences, with a platinum sheet as the counter electrode and a Ag/AgCl (3 M) as a reference electrode. All the measurements were carried out in a cell with 20 cm^3 (Metrohm) and in a nitrogen gas saturated atmosphere at 25 °C. The electropolymerization solutions contain 0.25 M pyrrole and (a) 0.12 M Na_2MoO_4 (J.T. Baker) + 0.35 M $NaNO_3$ (Biopack) or (b) 0.5 M NaSa (Sigma). Pyrrole (Sigma–Aldrich) was freshly distilled under reduced pressure before use.

Electrosynthesis of PPy films on steel electrodes was carried out by a potentiostatic technique. After the first electrosynthesis the film was rinsed carefully with distilled water.

The corrosion protection of the bilayer coatings was determined by open circuit potential (OCP)–time curves, potentiostatic and potentiodynamic measurements and electrochemical impedance spectroscopy (EIS) in 0.15 M NaCl (Merck) and 0.15 M HCl (J.T. Baker). The solutions were not deaerated during corrosion test measurements.

Electrochemical experiments were performed with a potentiostat–galvanostat Autolab/PGSTAT128N. EIS measurements were performed using a VoltaLab 40 Potentiostat PGZ301. The frequency used for the impedance measurements was changed from 100 kHz to 10 mHz, and the signal amplitude was 10 mV. ISI DS 130 SEM was used to examine the electrode surface characteristics.

Adhesion of bilayered PPy synthesized onto 316 L SS was tested using Scotch® Magic™ Tape 810 (3M). A piece of adhesive tape was pressed to the PPy film and pulled off. It was checked if the film was not removed at all, removed in patches or completely removed.

The concentrations of Fe and Mo in solution were determined using inductively coupled plasma atomic emission spectrometer (ICP-AES) Shimadzu 9000.

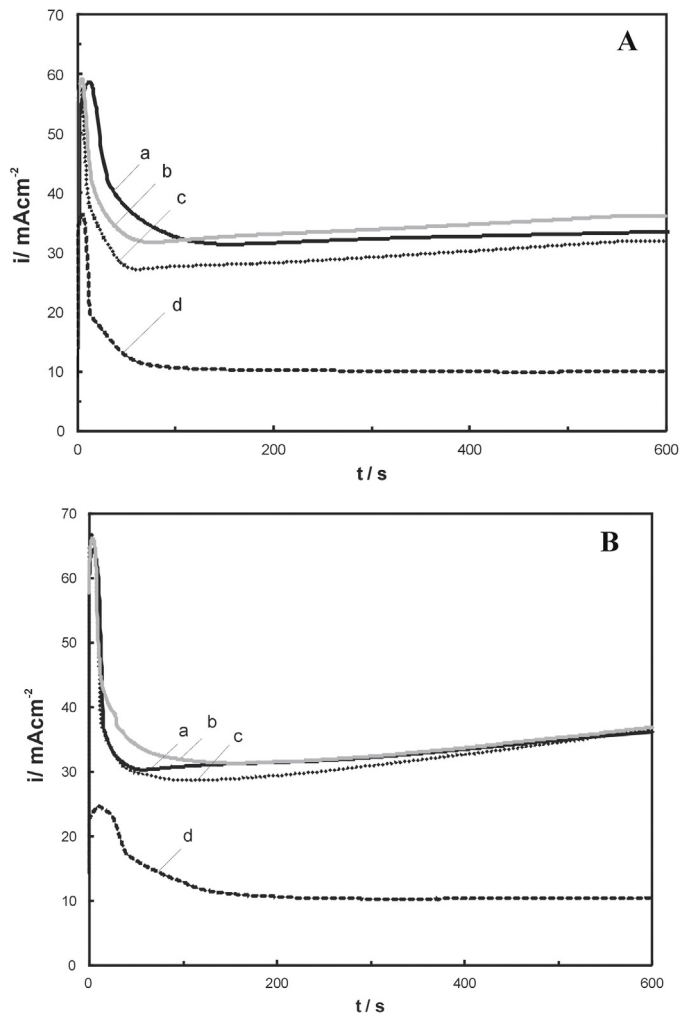

Fig. 1. Chronoaperometric curves corresponding to the electrosynthesis of an outer layer (PPy/Sa) obtained at 0.8 V vs. Ag/AgCl during 600 s in 0.5 M Sa containing 0.25 M Py. The inner layers were electrosynthesized at 0.8 V vs. Ag/AgCl in 0.12 M Na_2MoO_4 + 0.35 M $NaNO_3$ containing 0.25 M Py at pH 8 (A) and at pH 12 (B) during: (a) 180, (b) 300, (c) 480 and (d) 600 s.

3. Results and discussion

The first layer was electrodeposited at 0.8 V in 0.12 M Na_2MoO_4 + 0.35 M $NaNO_3$ at pH 8. The film was also prepared at pH 12 with all other parameters remained fixed including the electropolymerization charge. A gradual increase in current density was observed during the electropolymerization process at pH 8 or at pH 12 [15]. Molybdate and nitrate are incorporated as counter-ions into the synthesized film (PPy/MoO_4^{2-}–NO_3^-). After this, the second layer was electropolymerized at 0.8 V in 0.5 M Sa and 0.25 M Py (PPy/Sa) during 600 s, which are the experimental conditions that allow the formation of the hollow rectangular microtubes [7].

The inner layer was prepared with different electropolymerization times at pH 8 and at pH 12. The *i* vs. *t* transients obtained during the subsequent formation of the outer layer in Sa solution are presented in Fig. 1. First, current increases due to the growth of PPy with granular morphology and then decreases when HSa crystallizes on the electrode surface. Finally a current rise is observed which is associated with an increase in the number of growing microtubes as well as their height [7].

When the electropolymerization time for the PPy/MoO_4^{2-}–NO_3^- was 600 s, as we done in our previous work [15], the second layer formed in Sa solution only presents patches of deposits with rectangular morphology. This result is related with the high resistance of the first coating considering its high thickness. In order to find the optimum thickness of the inner layer, these films were electrodeposited at different times prior to PPy electrosynthesis in Sa solution. Then the electrodes covered by the bilayers were polarized in 0.15 M NaCl solution. The potentiodynamic runs are shown in Fig. 2 and for comparison, the curve of bare steel is also presented. The current rises in the case of the uncovered electrode at 0.35 V, denoting the onset of pitting corrosion. In the case of the covered samples, peaks associated with reversible and irreversible oxidation of the polymer were observed followed by current oscillations which appear at very positive potentials. After reversing the potential direction the characteristic loop of localized corrosion was observed (not shown in the figures). Thus, the covered electrodes can be polarized to high potentials without any sign of substrate dissolution. However for the thicker inner layers the shape of the potentiodynamic polarization curves is almost the same as that for the thinner one. So, we decided to use the coating formed during the shorter time of polymerization. That is, the electropolymerization times selected were 180 s and 600 s for the inner and outer layers, respectively. Both bilayers with the inner layer, PPy/MoO_4^{2-}–NO_3^-, formed

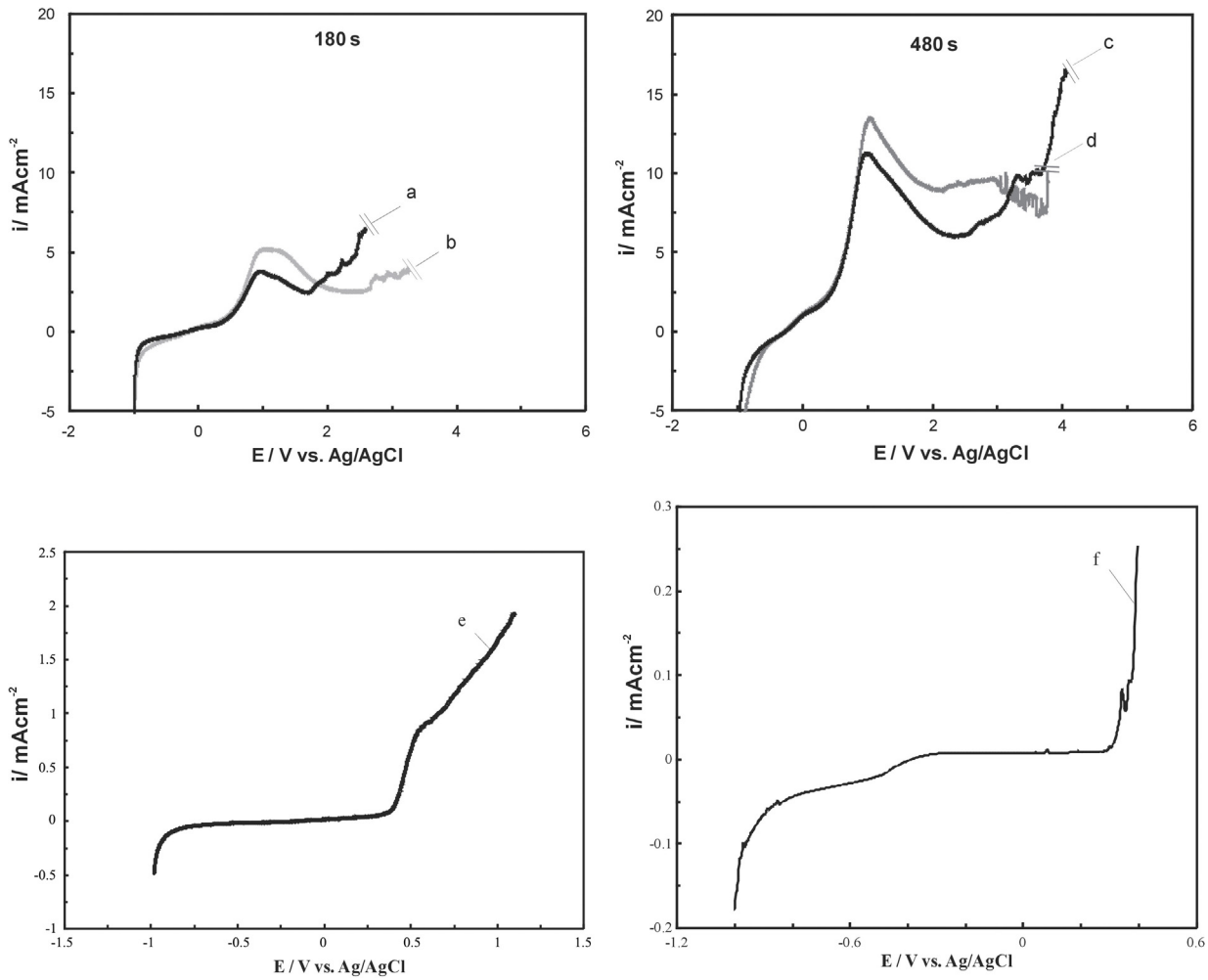

Fig. 2. Polarization curves registered in 0.15 M NaCl solution at 0.001 V s^{-1} for a steel electrode covered with an inner layer, PPy/MoO_4^{2-}–NO_3^-, formed at pH 8 (curves a and c) or at pH 12 (curves b and d), and with an outer layer, PPy/Sa. The inner and the outer layers were electrosythetized at 0.8 V vs. Ag/AgCl. The electropolymerization time of PPy/Sa was 600 s and those corresponding to PPy/MoO_4^{2-}–NO_3^- are indicated in the figure. The polarization curves corresponding to the steel electrode covered with a single layer of PPy/Sa (curve e) and for the uncoated steel (curve f) are also presented.

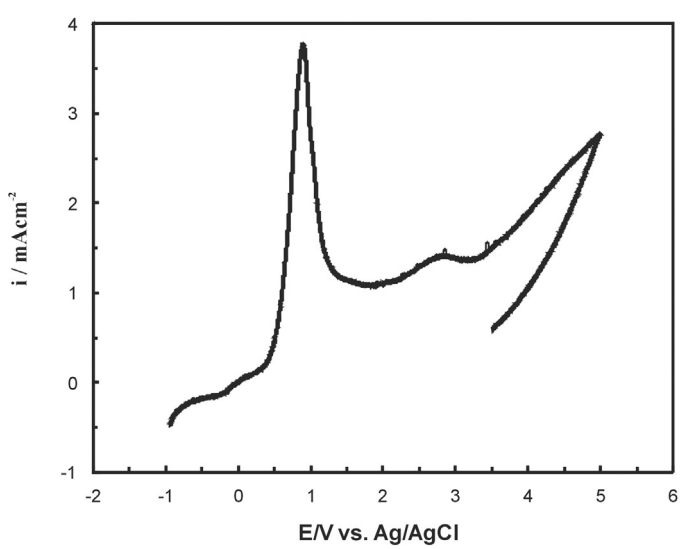

Fig. 3. Polarization curve registered in 0.15 M HCl solution at 0.001 V s^{-1} for a steel electrode covered with an inner layer, PPy/MoO_4^{2-}–NO_3^-, formed at pH 12, and with an outer layer, PPy/Sa. The inner and the outer layers were electrosythetized at 0.8 V vs. Ag/AgCl during 180 and 600 s respectively.

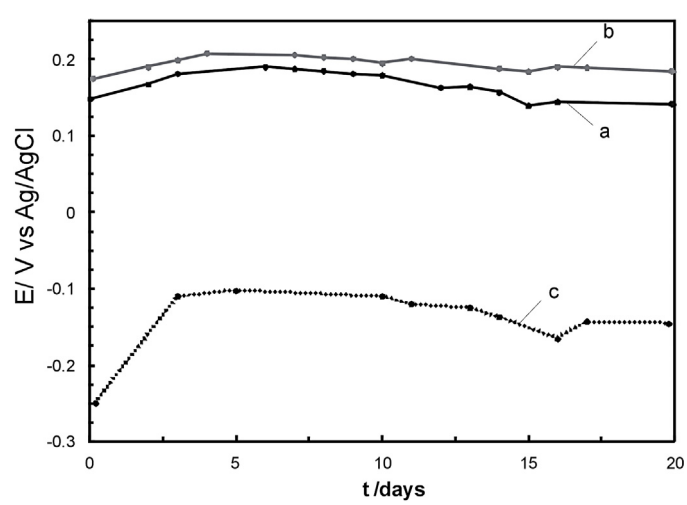

Fig. 4. Time dependence of the OCP in 0.15 M NaCl for a steel electrode covered with an inner layer, PPy/MoO_4^{2-}–NO_3^-, formed at pH 8 (a) or at pH 12 (b), and with an outer layer, PPy/Sa. The inner and the outer layer were electrosyntethized at 0.8 V vs. Ag/AgCl during 180 and 600 s respectively. The variation for the bare steel is also included.

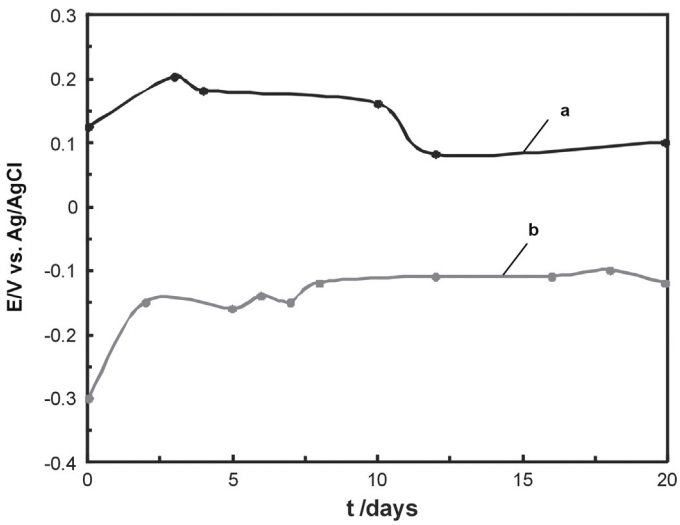

Fig. 5. Time dependence of the OCP in 0.15 M HCl for a steel electrode covered with an inner layer, PPy/MoO_4^{2-}–NO_3^-, formed at pH 12, and with an outer layer, PPy/Sa (a). The inner and the outer layer were electrosyntethized at 0.8 V vs. Ag/AgCl during 180 and 600 s respectively. The variation for a bare steel electrode is also included (b).

at pH 8 or at pH 12 were adherent and the films could only be removed by mechanical polishing.

For comparative purposes the curve corresponding to the steel covered only with the polymer synthesized in Sa solution is also presented (Fig. 2). The current rises approximately at 0.5 V denoting the onset of pitting corrosion. Thus, it can be concluded that this coating offers a lower corrosion protection compared with that obtained with the bilayers.

The shape of the curves obtained for the bilayers indicates that when the inner film was formed at pH 12 the pitting process initiates at more positive potentials (Fig. 2, curves b and d). Then, the protection imparted by this coating was also checked in 0.15 M HCl solution (Fig. 3). The current remained stable in the potential range analyzed and during the reverse scan no loop was formed. Thus, there are no signs of pitting corrosion even when very positive potentials were applied. On the other hand, the amount

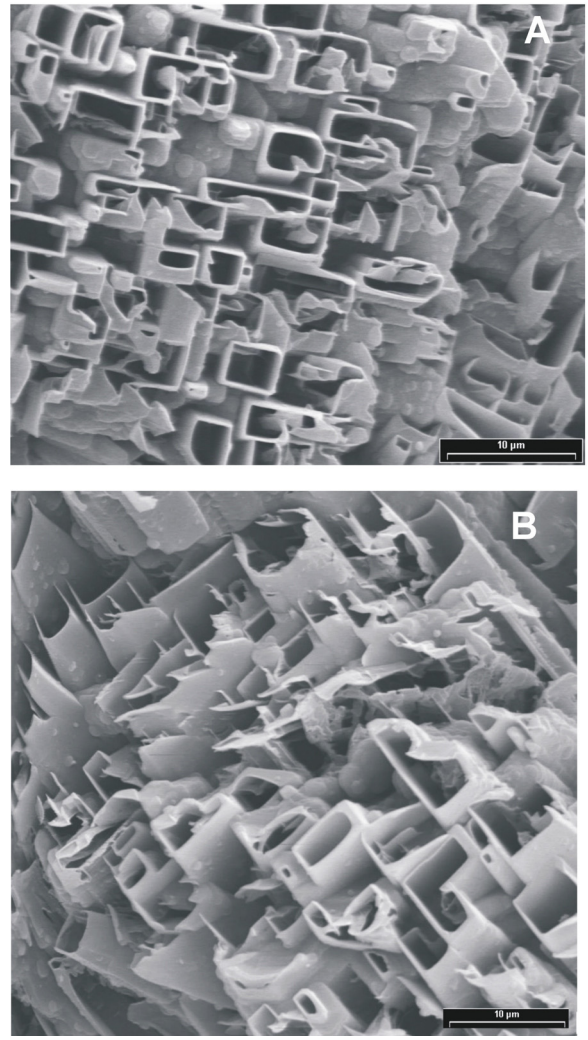

Fig. 7. SEM images obtained after 8 h of polarization at 0.6 V vs. Ag/AgCl in 0.15 M NaCl for a steel electrode covered with an inner layer, PPy/MoO_4^{2-}–NO_3^-, formed at pH 8 (A) or at pH 12 (B), and with an outer layer, PPy/Sa. The inner and the outer layer were electrosyntethized at 0.8 V during 180 and 600 s respectively.

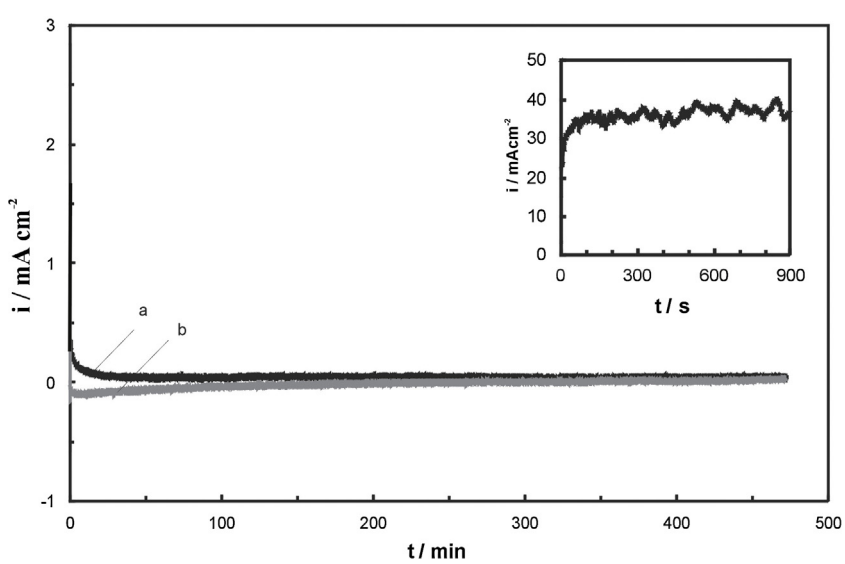

Fig. 6. Chronoamperometric curves obtained at 0.6 V vs. Ag/AgCl in 0.15 M NaCl solution for a steel electrode covered with an inner layer, PPy/MoO_4^{2-}–NO_3^-, formed at pH 8 (curve a) or at pH 12 (curve b), and with an outer layer, PPy/Sa. The inner and the outer layer were electrosyntethized at 0.8 V during 180 and 600 s respectively. The inset shows the response corresponding to the uncoated steel.

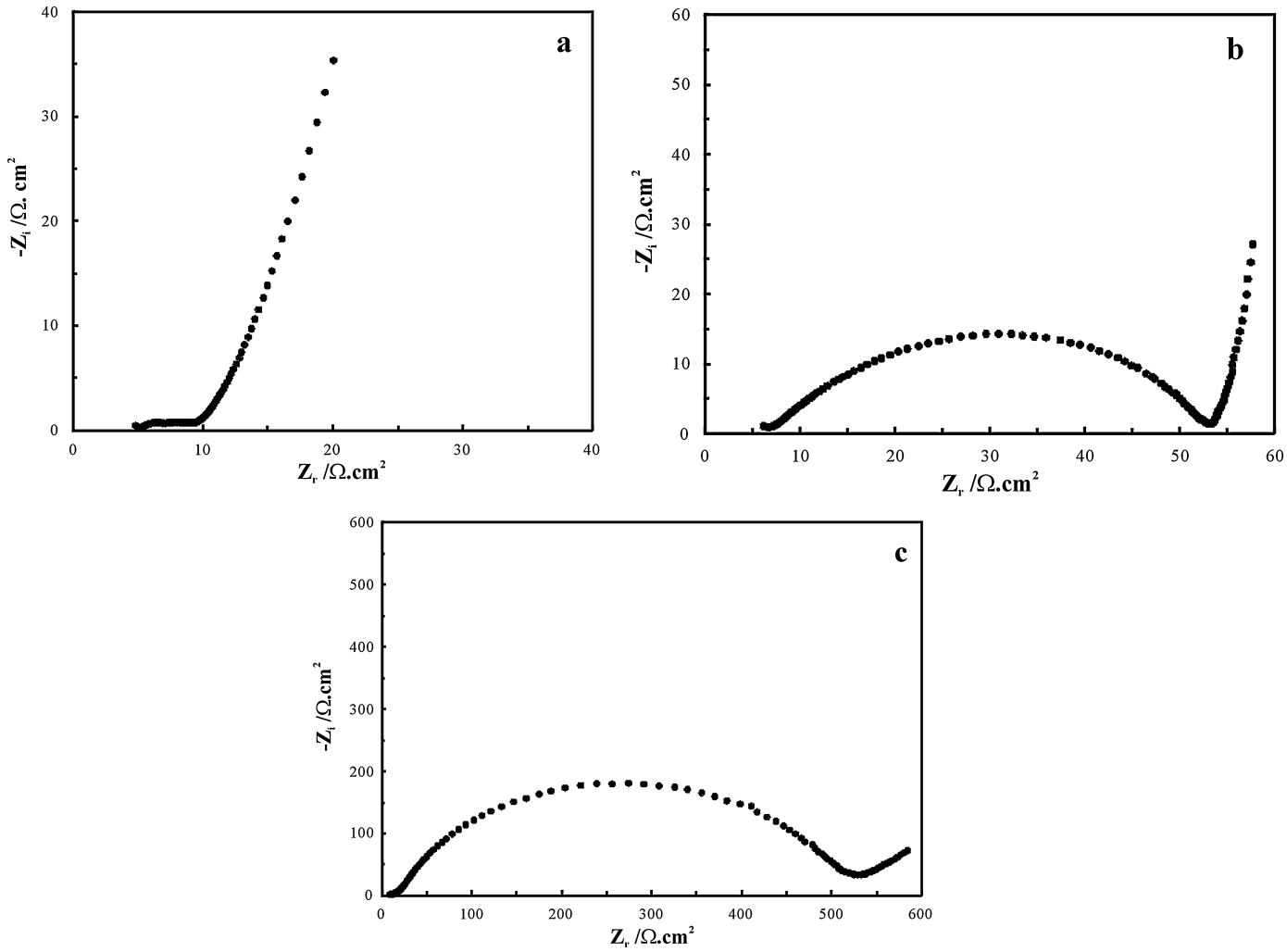

Fig. 8. Nyquist plots registered at OCP in 0.15 M NaCl solution for a steel electrode covered with an inner layer, PPy/MoO_4^{2-}–NO_3^-, formed at pH 8, and with an outer layer, PPy/Sa after: (a) 1, (b) 10 and (c) 20 immersion days. The inner and the outer layer were electrosyntethized at 0.8 V during 180 and 600 s respectively.

of integrated charge associated with the polymer redox process is lower than that obtained in neutral media.

The OCP variation with time for the steel covered with the bilayers in 0.15 M NaCl solution is presented in Fig. 4. The measured potentials are nobler than the potential of the uncoated steel (−0.14 V) even after 20 days of exposure. The quantity of Fe released after this period was 0.003 mg/L and less than 0.002 mg/L when the inner layer was synthesized at pH 8 and at pH 12, respectively. The bare electrode produced a Fe concentration of 1.200 mg/L. It can be concluded that there was no evidence of corrosion of the substrate.

Fig. 5 presents the evolution of the OCP as a function of time for the coating with the inner layer prepared at pH 12, but in this case in 0.15 M HCl solution. For comparative purposes the response of the uncoated electrode is also included. The OCP of the coated electrode remains at a value of approximately 0.12 V. Thus, the corrosion potential of the coated electrode is approximately 0.20 V higher than that of the uncoated electrode even after 20 days of immersion.

The protection imparted by the coatings was evaluated under more drastic conditions. At 0.60 V the pitting potential of the steel has been exceeded. The current measured for the samples coated with bilayers polarized at this potential indicates no occurrence of pitting corrosion even after 8 h of polarization (Fig. 6). After this period, the electrodes were examined using SEM (Fig. 7). The absence of any detectable change in the polymer surface indicates no occurrence of pitting corrosion. The results demonstrate that the coatings are an effective barrier to the diffusion of Cl^- ions and/or that the oxide film is repaired. The potentiostatic polarization in 0.15 M HCl solution of the coating with the inner layer prepared at pH 12 also indicates that a very good protection was achieved in acid media (not shown).

The corrosion resistance of the electrodes covered by the bilayers, whose inner layers were prepared at pH 12 or at pH 8, was evaluated by EIS. The Nyquist plots were recorded at various exposure times in neutral chloride solution under OCP conditions (Fig. 8 and Fig. 9). The diagrams are composed by a capacitive loop at high frequencies and a linear part at low frequencies. According to the model proposed by Koene et al. [19], which assumes that the reduction of the coating promotes the oxidation of the substrate, the experimental data can be fitted with the equivalent circuit depicted in Fig. 10. The results of the fitting are presented in Table 1. The errors of fitting are lower than 3% for all the parameters. In the circuit, R_S is the electrolyte solution resistance, R_{CT} is interpreted as the charge transfer resistance of the redox reaction of the polymer and CPE is the non-ideal double layer capacitance of the PPy/solution interface and it is defined as:

$$Z_{CPE} = \frac{1}{Y_0(j\omega)^n} \quad (1)$$

Table 1
Values for the parameters of the equivalent circuit obtained from the best fit to the impedance data in 0.15 M NaCl solution for PPy bilayers with an inner layer, PPy/MoO_4^{2-}–NO_3^-, electrosynthesized at pH 8 or at pH 12, and with an outer layer, PPy/Sa.

	t/days	R_s/Ω cm^2	Y_0/μF cm^{-2}	n	R_{CT}/Ω cm^2	R_W/Ω cm^2	s/Ω cm^2	α
PPy/MoO_4^{-2}–NO_3^-/pH 8	1	4.532	0.005	0.394	4.708	3.645	0.8	0.399
	10	6.636	1.6 E−4	0.65	47.26	0.68	0.265	0.452
	20	15.45	9.2E−5	0.711	907.8	0.007	1.1E−5	0.33
PPy/MoO_4^{-2}–NO_3^-/pH 12	1	3.986	0.0008	0.596	5.53	2.567	0.825	0.399
	10	5.82	0.0002	0.765	21.26	1.3	0.73	0.46
	20	7.56	0.0001	0.746	54.34	0.27	0.1	0.44

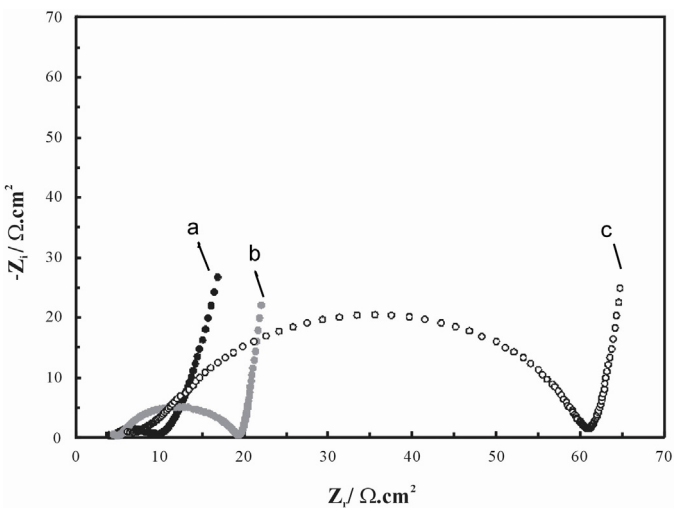

Fig. 9. Nyquist plots registered at OCP in 0.15 M NaCl solution for a steel electrode covered with an inner layer, PPy/MoO_4^{2-}–NO_3^-, formed at pH 12, and with an outer layer, PPy/Sa after: (a) 1, (b) 10 and (c) 20 immersion days. The inner and the outer layer were electrosyntethized at 0.8 V during 180 and 600 s respectively.

where j is the imaginary unit, n has the meaning of a phase shift with values between 0 and 1 and Y_0 is a constant with the dimension F cm^{-2} s^{n-1}.

Finally, W_0 is the finite-length Warburg impedance which accounts for diffusion of mobile charges in the polymer backbone and mobile anions throughout the PPy coating. It can be expressed as following:

$$W_0 = R_W \frac{\coth(j\omega s)^{\alpha}}{(j\omega s)^{\alpha}} \quad (2)$$

R_W represents the diffusion resistance and $s = \lambda^2/D$, where λ is the effective diffusion thickness and D is the effective diffusion coefficient of involved species. A transition from finite-length Warburg to semi-infinite Warburg behavior indicates that corrosive species can diffuse toward the substrate [19].

When the inner film was formed at pH 8 the R_{CT} significantly increases and the linear part tends to disappear as the immersion time goes on. Thus, the diffusional impedance has progressively a lower influence and the total impedance is controlled by the reaction rate of the redox process of the polymer. According to the model, the increase in R_{CT} was considered to be caused by a decrease in the reaction rate of the redox process of the polymer due to a loss of film conductivity. Differing from this behavior, the impedance diagram when the inner film was synthesized at pH 12 shows a less pronounced increase in the R_{CT} values. It can be also observed the diffusional process throughout the coating even after 20 days of immersion. Thus, this coating protects the steel more effectively than that with the inner layer formed at pH 8.

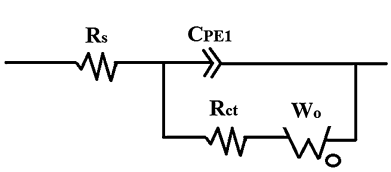

Fig. 10. Equivalent circuit proposed to simulate EIS results of coated samples. The significance of the parameters is given in the text.

The same type of impedance response was obtained during immersion in acid solution (Fig. 11). The values of the impedance parameters obtained from the fitting of the experimental data using the equivalent circuit shown in Fig. 10 are presented in Table 2. The data indicate that diffusional impedance controls the total impedance of the coating in the initial days of immersion. The changes in the impedance response during immersion show the same tendency as that observed in the neutral solution. That is, the charge transfer resistance of the redox reaction of the polymer (R_{CT}) increases, although the lineal behavior corresponding to the diffusional impedance is still appreciated after 20 days of immersion. EIS results demonstrated that the protective mechanism described for neutral solutions also operates for acid solutions.

Conducting polymer coatings have been reported to provide anodic protection to iron-based materials [20]. The polymer through a galvanic interaction is able to passivate a defect area where the bare substrate is directly in contact with the electrolyte. Reduction of the polymer as a result of this galvanic coupling with the substrate increases the resistance of the coating. EIS data indicate that the bilayer coating with the inner layer synthesized at pH 12 remains more electronically conducting during immersion in chloride solution. This result can be explained considering that the oxide formed at pH 12 is more effective in protecting the steel and then the polymer will be reduced more slowly. The results also indicated a very good performance of this coating in acid media.

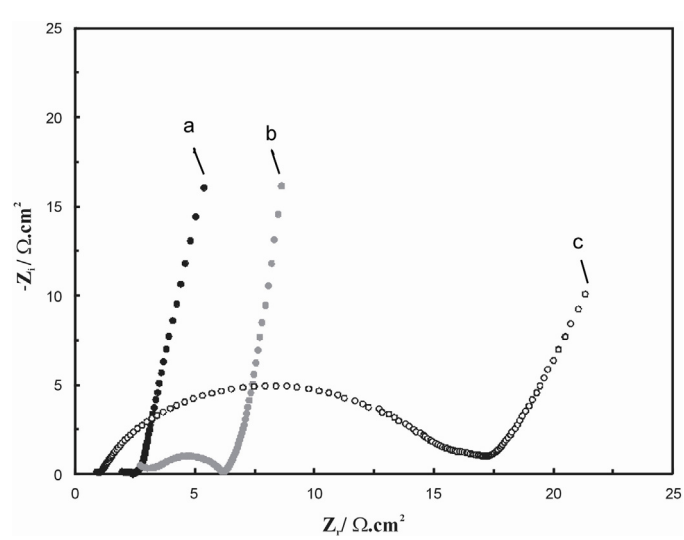

Fig. 11. Nyquist plots registered at OCP in 0.15 M HCl solution for a steel electrode covered with an inner layer, PPy/MoO_4^{2-}–NO_3^-, formed at pH 12, and with an outer layer, PPy/Sa, after: (a) 1, (b) 10 and (c) 20 immersion days. The inner and the outer layer were electrosyntethized at 0.8 V during 180 and 600 s respectively.

Table 2
Values for the parameters of the equivalent circuit obtained from the best fit to the impedance data in 0.15 M HCl solution for PPy bilayers with an inner layer, PPy/MoO_4^{2-}–NO_3^-, electrosynthesized at pH 12, and with an outer layer, PPy/Sa.

	t/days	$R_s/\Omega\,cm^2$	$Y_0/\mu F\,cm^{-2}$	n	$R_{CT}/\Omega\,cm^2$	$R_W/\Omega\,cm^2$	$s/\Omega\,cm^2$	α
PPy/MoO_4^{-2}–NO_3^-/pH 12	1	1.97	9.05E−5	0.820	0.410	0.905	0.450	0.449
	10	2.92	5.35E−5	0.662	3.22	0.927	0.391	0.44
	20	3.2	2.9 E−4	0.750	14.94	1.15	0.372	0.44

On the other hand, the ion transport through the bilayers of conducting polymers is conditioned by the characteristics of the dopant anions in both layers. The inner and the outer layer of a PPy bilayer can be doped with anions of good and limited mobility into the polymer matrix such as chloride and dodecylsulfate, respectively [21]. In this case, the oxidation process of the inner layer will be restricted because this process requires the diffusion of anions through the outer layer which is hindered due the size of its dopant anion. In our case, the transport of ions through the coating is not inhibited because cation and anion transport takes place during the charge and discharge of both polymer layers.

The corrosion protection performance of the bilayer coatings during a long immersion time in an aggressive medium can be explained by the following facts: (i) there are no big cracks or big pores in the coating; (ii) the penetration of Cl^- ions through the polymer layers is hindered because both salicylate and molybdate are relatively fixed in the PPy matrix; (iii) the transport through the bilayer is not blocked and the coating can act as an efficient oxidizer to maintain the steel in the passive state; (iv) the release of molybdate or nitrate from the polymer layer will help in protecting the steel.

4. Conclusions

In order to enhance the corrosion protection of 316 L SS coated by a PPy film with rectangular morphology, an inner layer of PPy was first grown by electrochemical deposition in a solution containing molybdate and nitrate. The experimental results indicated that the steel remained protected during a long exposure time in acid and neutral chloride solution. The bilayered coating presented also the ability to protect the substrate against localized corrosion. The capability of the films to provide an effective corrosion inhibition is explained by considering that the galvanic interaction between the polymer and the substrate together with the presence of molybdate near the electrode surface promote the maintenance of a passive oxide film. In addition, the penetration of chloride into the coating is hindered by the presence of molybdate and salicylate because of their low mobility. The coating with the inner layer formed in alkaline solution reduces the corrosion of the substrate more effectively than that formed in neutral solution, which is related to the more protective nature of the oxide formed at high pH values.

Acknowledgments

The Secretaría de Ciencia y Técnica-UNS, the Consejo Nacional de Investigaciones Científicas y Técnicas and the Agencia de Promoción Científica are gratefully acknowledged for the financial support.

References

[1] G.D. Sulka, K. Hnida, A. Brzózka, pH sensors based on polypyrrole nanowire arrays, Electrochim. Acta 104 (2013) 536–541.
[2] M. Beidaghi, C. Wang, Micro-supercapacitors based on three dimensional interdigital polypyrrole/C-MEMS electrodes, Electrochim. Acta 56 (2011) 9508–9514.
[3] M. Sharma, G.I.N. Waterhouse, S.W.C. Loader, S. Garga, D. Svirskis, High surface area polypyrrole scaffolds for tunable drug delivery, Int. J. Pharm. 443 (2013) 163–168.
[4] L. Santos, P. Martin, J. Ghilane, P.C. Lacaze, J.C. Lacroix, Micro/nano-structured polypyrrole surfaces on oxidizable metals as smart electroswitchable coatings, Appl. Mater. Interfaces 5 (2013) 10159–10164.
[5] B. Schulz, I. Orgzall, I. Díez, B. Dietzel, K. Tauer, Template mediated formation of shaped polypyrrole particles, Colloids Surf. A 354 (2010) 368–376.
[6] M.B. González, S.B. Saidman, Electrosynthesis of hollow polypyrrole microtubes with a rectangular cross-section, Electrochem. Commun. 13 (2011) 513–516.
[7] M.B. González, O.V. Quinzani, M.E. Vela, A.A. Rubert, G. Benítez, S.B. Saidman, Study of the electrosynthesis of hollow rectangular microtubes of polypyrrole, Synth. Met. 162 (2012) 1133–1139.
[8] N.K. Guimard, N. Gomez, C.E. Schmidt, Conducting polymers in biomedical engineering, Prog. Polym. Sci. 32 (2007) 876–921.
[9] R. Wadhwa, C.F. Lagenaur, X.T. Cui, Electrochemically controlled release of dexamethasone from conducting polymer polypyrrole coated electrode, J. Control. Release 110 (2006) 531–541.
[10] D. Svirskis, J. Travas-Sejdic, A. Rodgers, S. Garg, Electrochemically controlled drug delivery based on intrinsically conducting polymers, J. Control. Release 146 (2010) 6–15.
[11] M.B. González, L.I. Brugnoni, M.E. Vela, S.B. Saidman, Silver deposition on polypyrrole films electrosynthesized in salicylate solutions, Electrochim. Acta 102 (2013) 66–71.
[12] S. Biallozor, A. Kupniewska, Conducting polymers electrodeposited on active metals, Synth. Met. 155 (2005) 443–449.
[13] P.P. Deshpande, N.G. Jadhav, V.J. Gelling, D. Sazou, Conducting polymers for corrosion protection: a review, J. Coat. Tech. Res. 11 (2014) 473–494.
[14] U. Riaz, C. Nwaoha, S.M. Ashraf, Recent advances in corrosion protective composite coatings based on conducting polymers and natural resource derived polymers, Prog. Org. Coat. 77 (2014) 743–756.
[15] M.B. González, S.B. Saidman, Electrodeposition of polypyrrole on 316L stainless steel for corrosion prevention, Corr. Sci. 53 (2011) 276–282.
[16] R.-G. Hu, S. Zhang, J.-F. Bu, Ch.-J. Lin, G.-L. Song, Recent progress in corrosion protection of magnesium alloys by organic coatings, Prog. Org. Coat. 73 (2012) 129–141.
[17] U. Riaz, Ch. Nwaoha, S.M. Ashraf, Recent advances in corrosion protective composite coatings based on conducting polymers and natural resource derived polymers, Prog. Org. Coat. 77 (2014) 743–756.
[18] M.B. González, S.B. Saidman, Corrosion protection properties of polypyrrole electropolymerized onto steel in the presence of salicylate, Prog. Org. Coat. 75 (2012) 178–183.
[19] L. Koene, W.J. Hamer, J.H.W. de Wit, Electrochemical behaviour of poly(pyrrole) coatings on steel, J. Appl. Electrochem. 36 (2006) 545–556.
[20] T. Dung Nguyen, T. Anh Nguyen, M.C. Pham, B. Piro, B. Normand, H. Takenouti, Mechanism for protection of iron corrosion by an intrinsically electronic conducting polymer, J. Electroanal. Chem. 572 (2004) 225–234.
[21] J. Tamm, A. Alumaa, A. Hallik, V. Sammelselg, Redox properties of polypyrrole bilayers, Electrochim. Acta 46 (2001) 4105–4112.